Calculation of the Energy Band Diagram and Estimation of Electronic Transport Parameters of Metastable Amorphous $Ge_2Sb_2Te_5$

M. T. B. Kashem[a], S. Muneer[a,b], L. Adnane[a,c], F. Dirisaglik[a,d], A. Gokirmak[a], and H. Silva[a]

[a] Department of Electrical and Computer Engineering, University of Connecticut, Storrs, Connecticut 06269, USA
[b] Department of Electrical and Electronic Engineering, United International University, Dhaka 1212, Bangladesh
[c] Analog Devices, Boston, MA, USA
[d] Department of Electrical and Electronics Engineering, Eskisehir Osmangazi University, Eskisehir 26480, Turkey

We calculate critical electronic conduction parameters of the amorphous phase of $Ge_2Sb_2Te_5$ (GST), a common material used in phase change memory. We estimate the room temperature bandgap of metastable amorphous GST to be E_g (300K) = 1.84 eV based on a temperature dependent energy band model. We estimate the free carrier concentration at the melting temperature utilizing the latent heat of fusion to be 1.47 x 10^{22} cm^{-3}. Using the thin film melt resistivity, we calculate the carrier mobility at melting point as 0.187 $cm^2/V\text{-}s$. Assuming that metastable amorphous GST is a supercooled liquid with bipolar conduction, we compute the total carrier concentration as a function of temperature and estimate the room temperature free carrier concentration as p(300K) ≈ n(300K) = 1.69×10^{17} cm^{-3}. Free electrons and holes are expected to recombine over time and the stable (drifted) amorphous GST is estimated to have p-type conduction with p(300K) ≈ 6×10^{16} cm^{-3}.

Introduction

Phase change memory (PCM) is a high speed, high density non-volatile resistive memory technology that utilizes different phases (crystalline and amorphous) of phase change materials to store information (1,2). The material undergoes two types of switching phenomena: (i) Ovonic Threshold Switching (OTS), which causes the amorphous phase of the material to switch from a highly resistive state to a conductive state with application of high electric fields, resulting in substantial current flow and (ii) Ovonic Memory Switching (OMS), which is the non-volatile change of the phase of the material between amorphous and crystalline phases induced by heating (3). The chalcogenide alloy $Ge_2Sb_2Te_5$ (GST) is the most commonly used phase change material in PCM due to its rapid and repeatable phase change capability, high resistance contrast between amorphous and crystalline phases and high stability (4-8).

Though many studies have been reported regarding the atomic configuration (9-11) and optical properties (12,13) of GST, the electronic properties are still not well understood (14,15). In this work, we extract several electronic conduction parameters of amorphous

GST (a-GST) from experimental data. We use the activation energy of conduction (16) to calculate the temperature dependent energy band diagram of metastable a-GST assuming the energy bandgap shrinks linearly with temperature. We calculate the carrier concentration and mobility at the melting temperature from the reported latent heat of fusion of the material (17) and thin film melt resistivity (18). Assuming the carrier mobility to be weakly varying with temperature and bipolar conduction for the intrinsic material, we estimate the total carrier concentration in a wide temperature range using the device level measured resistivity for GST line cells (19).

Results and Discussion

Temperature dependent energy band model

We have previously determined the effective activation energy of conduction, E_a for metastable a-GST (16) (Figure 1a) utilizing the resistivity (ρ) versus temperature (T) data obtained from high-speed electrical measurements on nanoscale GST line cells (19). Using a reference $E_a = \frac{3}{2}k_BT$ at the melting temperature (T_{melt}), where k_B is the Boltzmann constant, we obtained $E_a = 0$ at ~ 930K, which we identified as the transition temperature from liquid-semiconducting to liquid-metallic phase of the material (T_{metal}). We have also constructed an energy band diagram assuming a linearly decreasing energy bandgap (E_g) with temperature and reference E_g = 1.09 eV at room temperature (20) and $\frac{3}{2}kT$ at T_{melt} (Figure 1b). Here, $E_{trap} = E_a + E_v$ where E_v is the valence band edge shows the energy level of the effective hole trap location assuming unipolar trap-limited band transport of holes. However, liquid GST is expected to have approximately the same number of electrons and holes generated during the crystalline to melt transition at T_{melt}. Since the behavior of the liquid GST and metastable a-GST display a continuum (19), bipolar conduction is expected to take place in metastable a-GST. Large defect concentration in a-GST (~10^{18}-10^{19} cm^{-3}) (21,22) gives rise to substantial localized trap states for electrons and holes in the energy bandgap which cause Fermi level (E_f) pinning around mid-bandgap ($E_g/2$) and consequently, a-GST appears as an intrinsic semiconductor (23-25). Moreover, we had previously assumed that the trap-to-band activation energy at melt is $\frac{3}{2}kT$ (Figure 1b), same as band-to-band activation, indicating E_{trap} to go above mid-gap ($E_g/2$) at ~500K and beyond. However, the hole traps are expected to exist between mid-gap and E_v (26) and additional electron traps are expected to exist between mid-gap and E_c. In this work, we demonstrate an analytical energy band model of metastable a-GST assuming intrinsic characteristics and utilizing the $E_a(T)$ model of (16).

We assume $E_g = \frac{3}{2}kT$ at T_{melt} and $E_a = E_g = 0$ at T_{metal} in accordance with the definition of T_{metal} (16). Furthermore, we assume same E_a for the emission of the trapped carriers from electron and hole traps ($E_{trap,electron} = E_c - E_a$, and $E_{trap,hole} = E_v + E_a$) and $\frac{dE_{trap,hole}}{dT} = \frac{dE_{trap,electron}}{dT} = 0$ at T_{metal} considering temperature independent E_{trap} near T_{metal}. $E_a(T)$ is given by (16),

$$E_a\,(T) = k_BT\left[\frac{E_{a,ref}}{k_BT_{ref}} + \alpha\left(T_{ref} - T\right)\right] \quad [1]$$

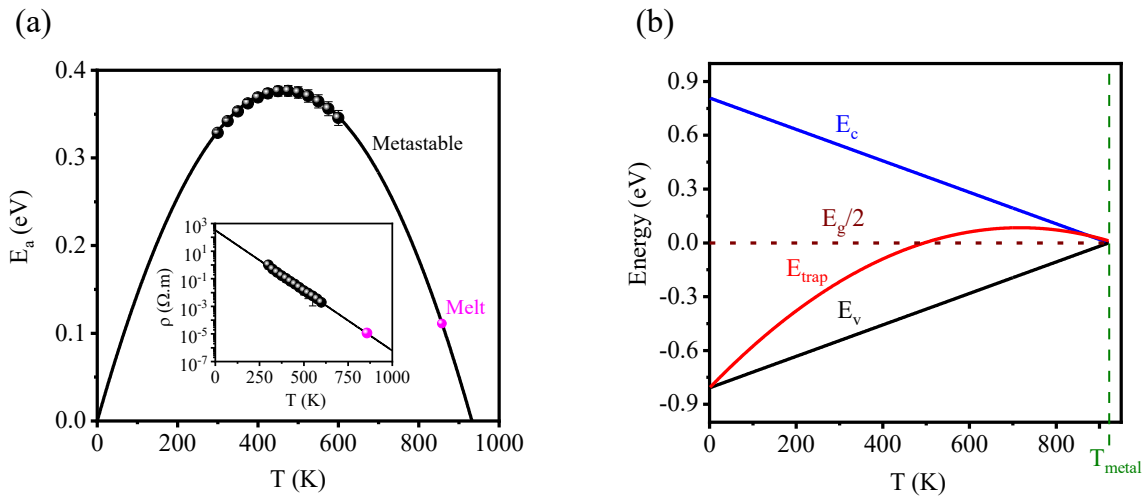

Figure 1. (a) Activation energy of metastable a-GST, E_a (●) (16) extracted from the measured resistivity, ρ(T) using device level high speed experiments on line cells (inset,●) (19). At T_{melt} (●), ρ is obtained from thin film measurements (18) and E_a is assumed to be $\frac{3}{2}kT$. (b) Constructed energy band diagram in (16). $E_{trap} = E_v + E_a$ is the effective hole trap location assuming the material to be predominantly p-type.

where α is the exponent of the exponentially decreasing model of ρ(T) (Figure 1a, inset) and $E_{a,ref}$ is the reference activation energy at the reference temperature, T_{ref}. Equation (1) can be simplified by replacing $E_{a,ref} = 0$ and $T_{ref} = T_{metal}$,

$$E_a\,(T) = \alpha k_B T (T_{metal} - T) \qquad [2]$$

$E_{trap,hole}$ can be expressed as (16),

$$E_{trap,hole}\,(T) = E_a(T) + E_v(T) = \alpha k_B T (T_{metal} - T) + aT + b \qquad [3]$$

where E_v is assumed to be a linear function of T,

$$E_v\,(T) = aT + b \qquad [4]$$

Using $E_c - E_g/2 = E_g/2 - E_v$ (assumption of symmetric band edges), taking mid-gap as the energy reference and band-gap disappearing at T_{metal} yields $E_v\,(T_{metal}) = 0$. Thus, we get from equation (4),

$$b = -aT_{metal} \qquad [5]$$

From equation (3), the assumption $\frac{dE_{trap,hole}}{dT} = 0$ at $T = T_{metal}$ leads to,

$$a = \alpha k_B T_{metal} \qquad [6]$$

Equation (3) can then be re-written using equation (5) and (6) as,

$$E_{trap,hole}\,(T) = -\alpha k_B T^2 + 2\alpha k_B T_{metal} T - \alpha k_B T_{metal}^2 \quad [7]$$

E_g at T_{melt} can be expressed as,

$$E_g(T_{melt}) = E_c - E_v = -2E_v = \frac{3}{2} k_B T_{melt} \quad [8]$$

Using equation (4)-(6), equation (8) can be written as,

$$2\alpha k_B T_{metal}^2 - 2\alpha k_B T_{metal} T_{melt} - \frac{3}{2} k_B T_{melt} = 0 \quad [9]$$

Solving equation (9) for $\alpha = 0.0202\ K^{-1}$ (19) and $T_{melt} = 858K$ (18) yields, $T_{metal} \sim 894K$, which is consistent with a previous study based on density functional/molecular dynamics simulations that showed liquid GST is metallic at 900K (27). We obtain room temperature bandgap of ~1.84 eV (Figure 2) which lies within the range of previously reported values for a-GST (3,28,29). If trap-assisted band-to-band generation is assumed to be sufficient to maintain a melt, $E_g(T_{melt})$ is $(E_{trap} - E_v) + (E_c - E_{trap}) = \frac{3}{2}kT_{melt} + \frac{3}{2}kT_{melt} = 3kT_{melt}$ instead of $E_g(T_{melt}) = 3kT_{melt}/2$, then T_{metal} comes out to be ~927K, which is in close agreement with our previous work (16).

Determination of electronic transport parameters

We calculate several electronic conduction parameters of a-GST based on experimental data. First, we determine the concentration of electron-hole pair (EHP) generated at T_{melt} from the latent heat of fusion (L_f) of GST which is the energy required to transition from

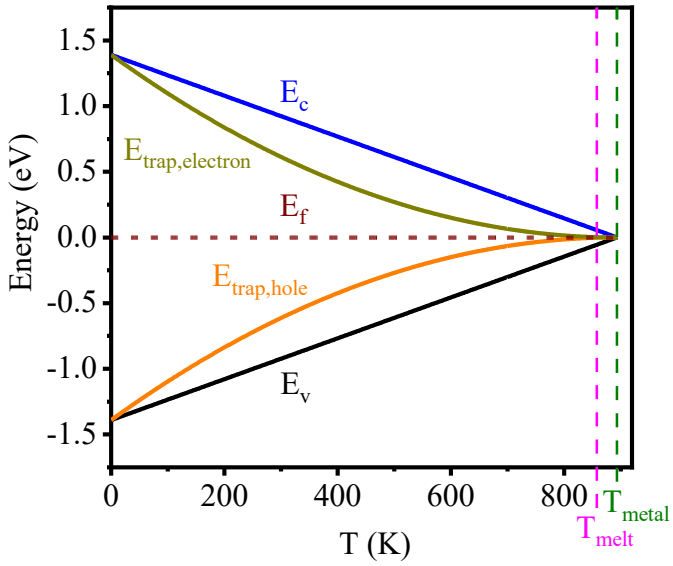

Figure 2. Calculated temperature dependent energy band model for metastable a-GST in this work. Electron traps capture free electrons from the conduction band and hole traps capture free holes from the valence band and the respective effective energy levels are given by, $E_{trap,electron}\,(T) = E_c(T) - E_a(T)$ and $E_{trap,hole}\,(T) = E_v(T) + E_a(T)$. T_{melt} = 858K as found in (18) and T_{metal} = 894K is obtained in this work.

solid to liquid phase. In terms of EHP, L_f can be described as the total energy of all generated EHP.

$$Energy\ of\ single\ EHP\ = K.E._{\cdot electron} + P.E._{\cdot electron} + K.E._{\cdot hole} + P.E._{\cdot hole} \quad [10]$$

where $K.E.$ and $P.E.$ stand for the kinetic energy and chemical potential energy respectively. $K.E.$ for both electron and hole is $\frac{3}{2}kT$ and $P.E.$ are given by,

$$P.E._{\cdot hole} = E_f - E_v \text{ and } P.E._{\cdot electron} = E_c - E_f \quad [11]$$

Therefore, equation (10) can be expressed as,

$$Energy\ of\ single\ EHP\ = \frac{3}{2}kT + E_c - E_f + \frac{3}{2}kT + E_f - E_v = 3kT + E_g \quad [12]$$

At T_{melt}, for $E_g\ = \frac{3}{2}kT_{melt}$,

$$energy\ of\ single\ EHP\ = \frac{9}{2}kT_{melt} \quad [13]$$

Using the reported L_f = 782 J/cm^3 (17), mass density of GST = 6200 kg/m^3 (30), and from equation (13), we obtain electron and hole concentration at melt, $n_{melt} = p_{melt} = 1.47\times10^{22}$ cm^{-3}. Besides, using molecular mass along with the mass density, we calculate the atomic density of GST to be ~3.26×10^{22} atoms/cm^3 which is ~2.2 times higher than n_{melt} and p_{melt}; suggesting the solid to liquid transition results in ~1 broken bond between 2 atoms.

We can estimate the carrier mobility at T_{melt} (μ_{melt}) using the melt resistivity measured for GST thin film (18). Electrical resistivity, ρ is given by,

$$\rho = \frac{1}{qn\mu_n + qp\mu_p} \quad [14]$$

where q is the electronic charge, n and p are electron and hole concentration respectively, μ_n and μ_p are electron and hole mobility respectively. Assuming $\mu_n \approx \mu_p = \mu$, μ_{melt} at T_{melt} for the intrinsic metastable a-GST (n = p) can be expressed from equation (14) as,

$$\mu_{melt} = \frac{1}{2\rho_{melt}qp_{melt}} \quad [15]$$

With our calculated p_{melt} and using ρ_{melt} from (18), we obtain μ_{melt} = 0.187 cm^2/V-s which is close to the previously reported value of 0.15 cm^2/V-s based on the estimation of density of states and average hole mobility in the extended valence band states and trap states (3). However, some other studies estimate the mobility to be in the range of ~10^{-2} – 10^{-3} cm^2/V-s (14,31,32). Experimental characterization of carrier mobility in drifted a-GST using Hall effect yields inconsistent results (26,33), possibly due to bipolar hopping conduction in complicated percolation paths and it is difficult to perform Hall measurements on metastable a-GST as high-sensitivity voltage measurements need to be performed in a short time-scale before the relaxation of the material and conductivity changes substantially.

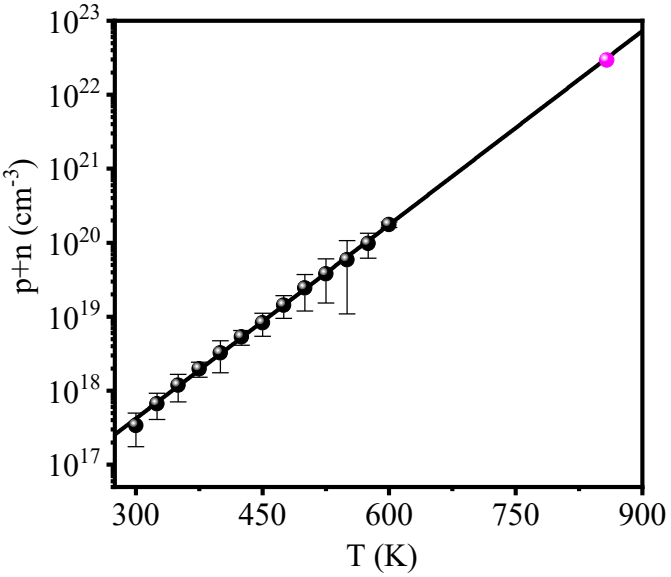

Figure 3. Sum of hole and electron concentration, (p+n) (●) calculated from the device level resistivity, ρ(T) (Figure 1, inset) assuming metastable a-GST as intrinsic semiconductor with $\mu_n \approx \mu_p = \mu_{melt}$. p+n at T_{melt} obtained from the latent heat of fusion is shown by (●).

We can also calculate the total carrier concentration, p+n at different temperatures using equation (14) and ρ(T) model from (19) assuming the carrier mobility to be a weak function of temperature (16) (we take $\mu(T) \sim \mu_{melt}$) (Figure 3):

$$p\,(T) + n(T) = \frac{1}{q\,\rho(T)\,\mu_{melt}} \qquad [16]$$

At room temperature, we obtain total carrier concentration of 3.37×10^{17} cm^{-3}, and hence hole concentration of 1.69×10^{17} cm^{-3}, which lies within the range of previously reported values of ~10^{17}-10^{18} cm^{-3} (14). Assuming that the carrier mobility does not change during resistance drift, and conduction in drifted aGST is dominated by hole transport, as observed in Seebeck measurements (18), the free hole concentration is expected to decline to ~6×10^{16} cm^{-3} over time based on the change in resistivity over time.

Conclusions

We have investigated several conduction parameters of metastable amorphous and liquid GST based on experimental results. We have constructed an energy band model for metastable a-GST assuming intrinsic behavior, calculated the semiconducting-liquid to metallic-liquid transition to be $T_{metal} \approx 894$K when band-gap drops to zero, and calculated the room temperature band-gap of metastable aGST as E_g (300K) = 1.84 eV. Assuming band-to-band generation of carriers during melting and from the latent heat of fusion, we have calculated free carrier concentrations $p(T_{melt}) \approx n(T_{melt}) = 1.47\times10^{22}$ cm^{-3} at the melting point, corresponding to approximately 1 broken bond per a pair of atoms. We have calculated effective carrier mobility at melt as $\mu_{melt} = 0.187$ cm^2/V-s, close to previously reported theoretical values. Assuming that the carrier mobility is insensitive to temperature and bipolar nature of conduction in liquid GST at T_{melt} is maintained in metastable a-GST

upon quenching, we estimate the room temperature carrier concentrations for metastable a-GST to be p(300K) ≈ n(300K) = 1.69×10^{17} cm^{-3}. We expect recombination of the free holes and electrons over time, leading to predominantly p-type conduction in drifted a-GST, with p(300K) ≈ 6×10^{16} cm^{-3}. These parameters are vital to model the electrical and thermal conductivity, current density, thermal boundary resistance and other related parameters in electro-thermal simulations of PCM devices.

Acknowledgements

The analysis was performed with the support of the US National Science Foundation (NSF) through Award ECCS 1711626. The experimental data used for this analysis were collected with the support of US NSF DMR-1710468 on devices fabricated with the support of US Department of Energy Office of Basic Energy Sciences.

References

1. S. W. Fong, C. M. Neumann, and H. S. P. Wong, *IEEE Trans. Electron Dev.*, **64**(11), 4374 (2017).

2. M. Le Gallo, and A. Sebastian, *J. Phys. D Appl. Phys.*, **53**(21), 213002 (2020).

3. A. Pirovano, A. L. Lacaita, A. Benvenuti, F. Pellizzer, and R. Bez, *IEEE Trans. Electron Dev.*, **51**(3), 452 (2004).

4. H. Lv, P. Zhou, Y. Lin, T. Tang, B. Qiao, Y. Lai, J. Feng, B. Cai, and B. Chen, *Microelectr. J.*, **37**(9), 982 (2006).

5. N. Yamada, E. Ohno, K. Nishiuchi, N. Akahira, and M. Takao, *J. Appl. Phys.*, **69**(5), 2849 (1991).

6. N. Ohshima, *J. Appl. Phys.*, **79**(11), 8357 (1996).

7. V. Weidenhof, I. Friedrich, S. Ziegler, and M. Wuttig, *J. Appl. Phys.*, **86**(10), 5879 (1999).

8. J. H. Kim, *J. Appl. Phys.*, **86**(12), 6770 (1999).

9. M. Naito, M. Ishimaru, Y. Hirotsu, and M. Takashima, *J. Non-cryst. Solids*, **345**, 112 (2004).

10. A. V. Kolobov, P. Fons, A. I. Frenkel, A. L. Ankudinov, J. Tominaga, and T. Uruga, *Nat. Mater.*, **3**(10), 703 (2004).

11. S. Shamoto, N. Yamada, T. Matsunaga, T. Proffen, J. W. Richardson Jr, J. H. Chung, and T. Egami, *Appl. Phys. Lett.*, **86**(8), 081904 (2005).

12. T. Ohta, and S. R. Ovshinsky, Photo-Induced Metastability in Amorphous Semiconductors, Edited by AV Kolobov, Chapter 18, Wiley-VCH, Weinheim (2003).

13. T. Nakai, T. Tsukamoto, S. Ashida, K. Yusu, N. Yoshida, K. Umezawa, N. Ohmachi, N. Morishita, N. Nakamura, and K. Ichihara, *Jpn. J. Appl. Phys.*, **43**(7S), 4987 (2004).

14. T. Kato, and K. Tanaka, K., *Jpn. J. Appl. Phys.*, **44**(10R), 7340 (2005).

15. M. Schumacher, H. Weber, P. Jóvári, Y. Tsuchiya, T. G. Youngs, I. Kaban, and R. Mazzarello, *Sci. Rep.*, **6**(1), 1 (2016).

16. S. Muneer, J. Scoggin, F. Dirisaglik, L. Adnane, A. Cywar, G. Bakan, K. Cil, C. Lam, H. Silva, and A. Gokirmak, *AIP Adv.*, **8**(6), 065314 (2018).

17. Z. Fan, and D. E. Laughlin, D.E., *Jpn. J. Appl. Phys.*, **42**(2S), 800 (2003).

18. L. Adnane, F. Dirisaglik, A. Cywar, K. Cil, Y. Zhu, C. Lam, A. F. M. Anwar, A. Gokirmak, and H. Silva, *J. Appl. Phys.*, **122**(12), 125104 (2017).

19. F. Dirisaglik, G. Bakan, Z. Jurado, S. Muneer, M. Akbulut, J. Rarey, L. Sullivan, M. Wennberg, A. King, L. Zhang, and R. Nowak, *Nanoscale*, **7**(40), 16625 (2015).

20. Y. Kim, K. Jeong, M. H. Cho, U. K. Hwang, H. S. Jeong, and K. Kim, *Appl. Phys. Lett.*, **90**(17), 171920 (2007).

21. A. K. Jonscher, and C. K. Loh, *J. Phys. C Solid State,* **4**(11) 1341 (1971).

22. D. Ielmini, and A. L. Lacaita, *Mater. Today* **14**(12) 600 (2011).

23. D. Ielmini, D. Sharma, S. Lavizzari, and A. L. Lacaita, (2008, April). In *2008 IEEE International Reliability Physics Symposium* 597 (2008).

24. M. Le Gallo, and A. Sebastian, *J. Phys. D Appl. Phys.* **53**(21) 213002 (2020).

25. D. Ielmini, *Phase Change Memory: Device Physics, Reliability and Applications.*, A. Redaelli, Editor, p. 15, Springer (2018).

26. J. Luckas, D. Krebs, S. Grothe, J. Klomfaß, R. Carius, C. Longeaud, and M. Wuttig, *J. Mater. Res.*, **28**(9), 1139 (2013).

27. J. Akola, and R. O. Jones, *J. Phys.-Condens. Mat.*, **20**(46), 465103 (2008).

28. E. Garcıa-Garcıa, A. Mendoza-Galvan, Y. Vorobiev, E. Morales-Sanchez, J. Gonzalez-Hernandez, G. Martınez, and B. S. Chao, *J. Vac. Sci. Technol. A: Vacuum, Surfaces, and Films*, **17**(4), 1805 (1999).

29. H. B. Yao, L. P. Shi, T. C. Chong, P. K. Tan, and X. S. Miao, *Jpn. J. Appl. Phys.*, **42**(2S), 828 (2003).

30. S. Harnsoongnoen, C. Sa-Ngiamsak, and A. Siritaratiwat, *Int. J. Mod. Phys. B,* **23**(17), 3625 (2009).

31. H. Y. Wu, W. Wang, and W. J. Lu, *Phys. Status Solidi B,* **253**(9) 1855 (2016).

32. T. Gotoh, *Can. J. Phys.* **92**(7/8) 681 (2014).

33. L. Xu, L. Tong, L. Geng, F. Yang, J. Xu, W. Su, D. Liu, Z. Ma, and K. Chen. *J. Appl. Phys.*, **110**(1) 013703 (2011).